Original Article

The TrkB agonist, 7,8-dihydroxyflavone, impairs fracture healing in mice

Maddison R. Johnstone[1], Rhys D. Brady[2], Jarrod E. Church[1], David Orr[1], Stuart J. McDonald[1,2]*, Brian L. Grills[1]*

[1]Department of Physiology, Anatomy and Microbiology, School of Life Sciences, La Trobe University, Melbourne, Australia;
[2]Department of Neuroscience, Central Clinical School, Monash University, Melbourne, Australia
* equal contribution

Abstract

Objectives: To study the effects of the selective TrkB agonist, 7,8-dihydroxyflavone (7,8-DHF), on fracture healing in mice and on an osteoprogenitor cell line, Kusa4b10, *in vitro*. **Methods**: Mice received unilateral closed mid-shaft tibial fractures and treated for two weeks with vehicle or 5 mg/kg/day DHF and euthanised at 28 days post-fracture. Calluses were analysed by micro-computed tomography (μCT) and three-point bending biomechanical test. Kusa4b10 cells were cultured with 50nM of 7,8-DHF or vehicle for 3-, 7-, 14-days for RT-PCR, and 21 days for mineralization. **Results**: μCT found 7,8-DHF calluses had decreased tissue volume (p=0.042), mean polar moment of inertia (p = 0.004), and mean cross-sectional area (p=0.042) compared to controls. At 28 days biomechanical analyses showed 7,8-DHF treatment decreased peak force (p=0.011) and stiffness per unit area (p=0.012). 7,8-DHF treatment did not change Kusa4b10 gene expression of Runx2 and alkaline phosphatase at all time points, nor mineralization. **Conclusions**: 7,8-DHF treatment had a negative impact on fracture healing at 28 days post-fracture via an unknown mechanism. 7,8-DHF may have had a central role in impairing fracture healing.

Keywords: 7,8-DHF, BDNF, Bone, Fracture, TrkB Agonist

Introduction

Fractures are an extremely common injury of the skeletal system, with the residual lifetime risk of a minimal trauma fracture approximately 44% for women and 25% for men over the age of 60 in Australia[1]. To date, there are very few effective non-surgical treatments to aid in the healing of fractures, and to prevent malunion and non-union of fractures, a complication that affects approximately 5-10% of patients worldwide[2,3]. Two non-surgical approaches that are being developed to clinically enhance fracture healing

are biophysical enhancement e.g. electromagnetic field stimulation, and low-intensity pulsed ultrasonography[4-7], and biological enhancement e.g. therapeutic use of vascular and osteogenic growth factors, stem-cells, and morphogenic molecules to aid bone regeneration[4,8]. Identifying novel molecules that promote some of the key biological events of fracture healing, including angiogenesis and innervation, required for proper fracture healing, appear to have the greatest potential to improve bony repair.

Circulating neurotrophic factors are a branch of osteogenic stimulating peptides that have such potential. Neurotrophins are up-regulated in a variety of repairing tissues with evidence to suggest that they have important roles during angiogenesis[9-12] and inflammation[13-16], which are two key processes in fracture healing[17]. Specifically, the neurotrophin, nerve growth factor (NGF) and signalling via its receptor, TrkA, have been shown to stimulate osteoblastic mineralization and improve the mechanical properties of healing bone fractures[18-20]. Another neurotrophic factor that has recently been shown to have a role in fracture healing is brain derived neurotrophic factor (BDNF). Since its discovery

in 1982, BDNF has been established as an important modulator of synaptic plasticity and pruning in the central nervous system (CNS) via two pathways; high affinity TrkB (pro-survival) and low affinity p75NTR (pro-apoptotic)[21-24]. Several studies in rodents and humans have identified high levels of BDNF and its receptor, TrkB, in and around the site of fracture healing[25-27]. Gene and protein expression of BDNF and TrkB were markedly elevated in chondrocytes and active osteoblasts in proliferating and mature zones of the endochondral ossification front in 7-week old rats[28]. Furthermore, BDNF gene expression was elevated in callus tissue 28 days post-osteotomy in rats, which is the transition period of cartilaginous callus being replaced by woven bone, as well as remodelling of woven bone to lamellar bone[29,30]. Location of BDNF and TrkB in the inflammatory phase of fracture healing and soft callus stages where endochondral ossification begins, may indicate that BDNF has an important, early role in bone healing via endochondral ossification and intramembranous ossification.

One of the important processes that drives the transition of cartilage to woven bone, and remodelling of callus is re-establishment of blood vessels. BDNF has been shown both *in vitro* and *in vivo* to stimulate endothelial cell migration, proliferation and formation of new blood vessels[9,10,25,31] largely by increasing the production of vascular endothelial growth factor (VEGF)[32]. Another mechanism through which BDNF may also promote fracture healing is via the up-regulation of ossification proteins ALP and BMP-2 in osteoblasts, with BDNF treatment found to upregulate both ALP and BMP-2 in cementoblasts, a tooth root enamel mineralizing cell type similar to osteoblasts[33]. *In vitro*, BDNF has been identified in osteoblastic MC3T3-E1 cells[34] however, an osteoblastic response to BDNF treatment has yet to be described in the literature. Taken together, these findings suggest that BDNF may have an active role in fracture callus and healing, possibly by mediating angiogenesis and promoting bone formation, however, there are no studies investigating topical or systemic administration of BDNF, or activation of its receptor TrkB during fracture healing. Since BDNF can stimulate both pro-survival and pro-apoptotic pathways, it is not an appropriate choice of molecule to investigate the sole signalling pathway of BDNF and TrkB. Small novel molecules have been identified to target and potently activate only TrkB including 7,8-dihydroxyflavone (7,8-DHF)[35].

7,8-DHF is a flavonoid derivative with antioxidant and anti-inflammatory effects[35-39] and has been shown to potently activate the TrkB receptor[35,36,40]. Doses of 5 mg/kg/day of 7,8-DHF strongly activated TrkB receptors in BDNF knockout mice[35]. Additionally, 7,8-DHF reduced neuronal apoptosis and inflammation in rodent models subjected to traumatic brain injury (TBI) at a dose of 5 mg/kg/day[35,38,40,41]. 7,8-DHF is well tolerated in rodent models of TBI[36,38], depression[37], Alzheimer's disease[42,43], aging[44] and stress[45], with no detrimental effects reported in mice, however, to our knowledge, there has been no data describing the effects of 7,8-DHF on the skeletal system. Therefore, on assessing all the previous literature, it is hypothesized that 7,8-DHF treatment should have a positive effect on fracture healing. In the current experiments, effects of 7,8-DHF on the structural and biomechanical features of healing fractures in mice, murine bone growth, and osteoblastic differentiation and mineralization *in vitro* were investigated.

Methods

Animals

Thirty C57BL/6 male mice were supplied by the Australian Animal Resource Centre (ARC, Western Australia). Mice were 12 weeks of age at the time of experimentation and were housed individually during the experiment under a 12 h light/dark cycle with access to water and food *ad libitum*. All experimental procedures were approved by the La Trobe Animal Ethics Committee (AEC 17-05), were within the guidelines of the Australian code of practice for the care and use of animals for scientific purposes by the Australian National Health and Medical Research Council, and in compliance with the ARRIVE guidelines for how to report animal experiments.

Experimental groups

All mice received unilateral tibial fractures. To assess the effects of TrkB agonist, 7,8-DHF on fracture healing, mice were randomly allocated to receive either vehicle (30% Kolliphor® HS 15 in 0.1M sodium phosphate buffer; *n*=15) or 7,8-DHF in vehicle (*n*=15). Kolliphor® HS 15 was used as vehicle due to the poor water solubility of 7,8-DHF. A microemulsion of 7,8-DHF was used made in 30% Kolliphor® HS 15 in 0.1M sodium phosphate buffer. Kolliphor® HS 15 is white, odourless emulsifying agent commonly used in human and veterinary injection formulations[46-50]. Intraperitoneal injections of 7,8-DHF (5 mg/kg/day) or vehicle were given daily for 14 days post-injury. Previous research has shown this regimen of 7,8-DHF was effective at activating TrkB receptors centrally and peripherally[36,39,41-43]. All mice were euthanised via carbon dioxide asphyxiation at 28 days post-fracture. Nine mice were excluded from analysis; 7 due to tibial/fibular fusions, 2 due to already broken on analysis.

Closed tibial fracture model

Tibial fractures were performed using previously described standard protocols[51-55]. The fracture model is a closed, internally fixated fracture of the right tibial mid-shaft. In brief, under isoflurane anaesthesia, a 5 mm incision was made in the skin superficial to the anteromedial tibial surface, distal to the knee joint. Periosteal tissue was removed and an entry point into the tibial shaft was made using a 26-gauge hypodermic needle. An intramedullary rod was inserted down into the medullary canal of the tibia, and a mid-tibial fracture was made using a pair of modified skin staple removers. An X-ray of the tibia was performed to confirm fracture using DEXCOWIN® portable X-ray device (DEXCOWIN Co., Ltd. Pasadena, CA, USA). The intramedullary rod was removed

and replaced with a larger stabilising rod, and another X-ray was performed to confirm rod and fracture position. Incisions were closed using 5-0 synthetic surgical suture. Mice were given 5 mg/kg of Carprofen (RIMADYL®; Zoetis, Parsippany, NJ) and Buprenorphine (0.1 mg/kg) for pain relief.

Micro-computed tomography (μ CT)

μCT was performed on fractured tibial calluses. Fractured tibiae were immersed in fixative (4% paraformaldehyde in 0.1M sodium cacodylate buffer) for 48 h then stored in 10% sucrose in 0.1M sodium cacodylate buffer at 4°C until use. Scanning of tibiae was performed using SKYSCAN 1076 *in vivo* X-ray micro-computed tomography (Bruker-microCT) in 70% ethanol with acquisition parameters of 9 μm voxel resolution, 0.5 mm aluminium filter, 48 kV voltage, 100 μA current, 2,400 ms exposure, rotation 0.5° across 180°, frame averaging of 1. Images were reconstructed using NRecon (V1.6.3.1) with the following parameters: smoothing factor, 1; ring artefacts, 6; beam-hardening corrections, 35%; pixel defect mask, 5%; C.S rotation, 0; and misalignment compensation, <3. Images were realigned and orientated using Dataviewer (V1.4.4) to obtain transaxial datasets for calluses. Analysis of the transaxial datasets was performed using CTAn (V1.11.8.0) and the region of interest (ROI) was identified as 300 slices (i.e. 150 slices proximal and distal to the fracture line of the callus); the border of the callus was manually traced. Thresholds used for parameter quantification were determined using the automatic "otsu" algorithm within CTAn and visual examination of unreconstructed X-ray images. A grayscale adaptive threshold of 41-255 was used for structural analysis of calluses 28-days post-fracture. 2D and 3D data, and 3D models were generated and the following parameters were used for structural analysis of callus: total callus volume (TV); new mineralized bone tissue volume (BV), bone fractional volume (BV/TV), mean polar moment of inertia (MMI), bone surface (BS) and mean cross sectional area (T.Ar).

Biomechanical assessment of fracture calluses

Following μCT analysis, a three-point mechanical bending test was performed on calluses 28-day post-fracture to assess the potential effect of 7,8-DHF treatment of the biomechanical properties of bone. Samples were equilibrated at room temperature on the day of assessment. Each tibia was mounted onto an 8 mm stabilising platform in a mediolateral position. A 200 N force transducer descended at a constant rate of 1.67 mm/sec and loaded each callus centrally. A load-displacement (x-y) graph was plotted and force (g) and deflection (mm) values were recorded. Biomechanically disrupted callus ends were imprinted onto dental wax. Magnified imprints were imaged using Leica DFC420 light microscope (Leica Microsystems Ltd., Heerbrugg, Switzerland) connected to Leica IM50 imaging software (Leica). Cross sectional areas measured using Leica Qwin V3 Standard software (Leica). Differences in peak force

Table 1. Oligonucleotide name and sequence (5'-3') used in Real-Time PCR.

Oligonucleotide name	Sequence (5'3')
mGAPDH	Sense - AATCTCCACTTTGCCACTG
	Anti-sense - CCTCGTCCCGTAGACAAAA
mRunx2	Sense – AGCAACAGCAACAACAGCAG
	Anti-sense – GTAATCTGACTCTGTCCTTG
mAlkaline phosphatase	Sense – AAACCCAGACACAAGCATTCC
	Anti-sense - TCCACCAGCAAGAAGCC
PCR, polymerase chain reaction; GAPDH, glyceraldehyde 3-phosphate dehydrogenase	

to failure, load per unit area, stiffness and stiffness per unit area were calculated from the deflection data.

Cell culture

Cell culture was used to investigate the effects of 7,8-DHF on osteoblastic cell line, Kusa4b10. Kusa4b10 cells are a genetic sub-clone of multi-potential bone marrow stromal cells, Kusa O[56], and have demonstrated a more osteoblastic phenotype than Kusa O cells, thus more suitable for investigations on osteoblastic differentiation[56,57]. Cells were cultured in α-MEM (Gibco® Life Technologies™, Auckland, NZ), supplemented with 10% Australian Premium Foetal Bovine Serum (FBS) (Australian Ethical Biologicals Pty. Ltd., Coburg, AU) and used between passages 10-16. All cultures were maintained in an incubator at 37°C in 5% CO_2 and 95% O_2. For these experiments, in order to gain an insight into the role BDNF has on fracture healing the influence of 7,8-DHF on osteoblastic marker expression, as well as mineralization was investigated. For studies that required Kusa4b10 cell differentiation, including RT-PCR and mineralisation studies, cells were sub-cultured at a density of 3000 cells/ml in α-MEM + 10% FBS for 3 days, after which medium was aspirated and cells were cultured in osteoblastic differentiation medium, containing α-MEM + 10% FBS supplemented with 50 μg/ml ascorbate and 10mM β-glycerophosphate[48,56,57]. Medium was replenished three times a week.

Real-time Polymerase Chain Reaction (RT-PCR)

Kusa4b10 cells were cultured in osteoblastic differentiation medium and treated with 50nM of 7,8-DHF (based on pilot research) or vehicle. The medium was replaced three times per week. Cells were isolated at three different timepoints; 3-, 7-, and 14-days. These three timepoints were chosen because they reflect three stages of Kusa4b10 cell differentiation, are similar timepoints used in the current studies investigating Kusa4b10[56-59]. Total RNA was prepared using PureZOL™ (Bio-Rad Laboratories Inc., Hercules, USA). RT-PCR was performed as previously described[18,48]. Briefly, reverse transcription was performed from 1 μg of total RNA
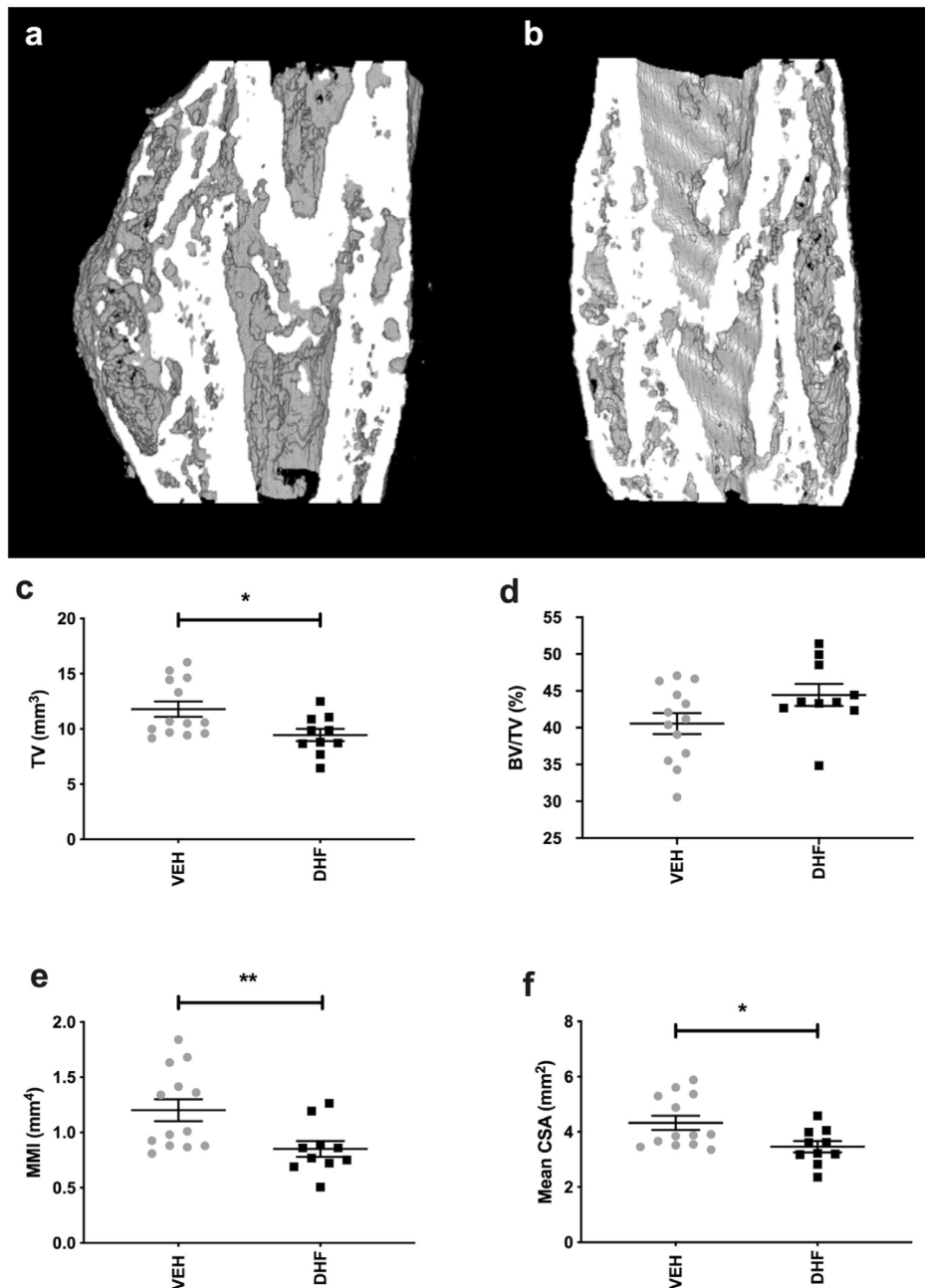
Figure 1. Effects of 7,8-DHF treatment on 28-day callus structural parameters using μCT. Longitudinal mid-point images representative of 300 slice reconstructed hemi-callus (a-b). 7,8-DHF treatment decreased total callus volume (TV, c; *p=0.042), mean polar moment of inertia (MMI, e; **p=0.004) and mean cross-sectional area of callus (CSA, f; *p=0.047) at 28 days post-fracture compared to vehicle treatment. 7,8-DHF; 7,8-dihydroxyflavone. BV/TV; bone fractional volume. Bars are mean ± SEM, n=9-12/group.

using iScript™ cDNA Synthesis Kit (Bio-Rad). Glyceraldehyde 3-phosphate dehydrogenase (GAPDH) was used as an internal control gene. RT-PCR was performed in triplicate using SsoFast™ EvaGreen® Supermix (Bio-Rad) and specific oligonucleotide primers (Table 1) on an iQ 96-well PCR system (Bio-Rad). Each amplification reaction contained 1 μl of cDNA and 300 nM of primer. Thermal cycling conditions included initial denaturation at 95°C for 30 s, followed by 40 cycles of 95°C for 5 s and 55°C for 5 s. Melt-curve analysis was performed post-cycling to confirm specificity of the amplified products. Relative quantification of genes of interest mRNA expression normalised to the house-keeping gene and was determined using the $2^{-\Delta\Delta Ct}$ method. Specific oligonucleotide primers (Table 1) were Runx2; a marker of
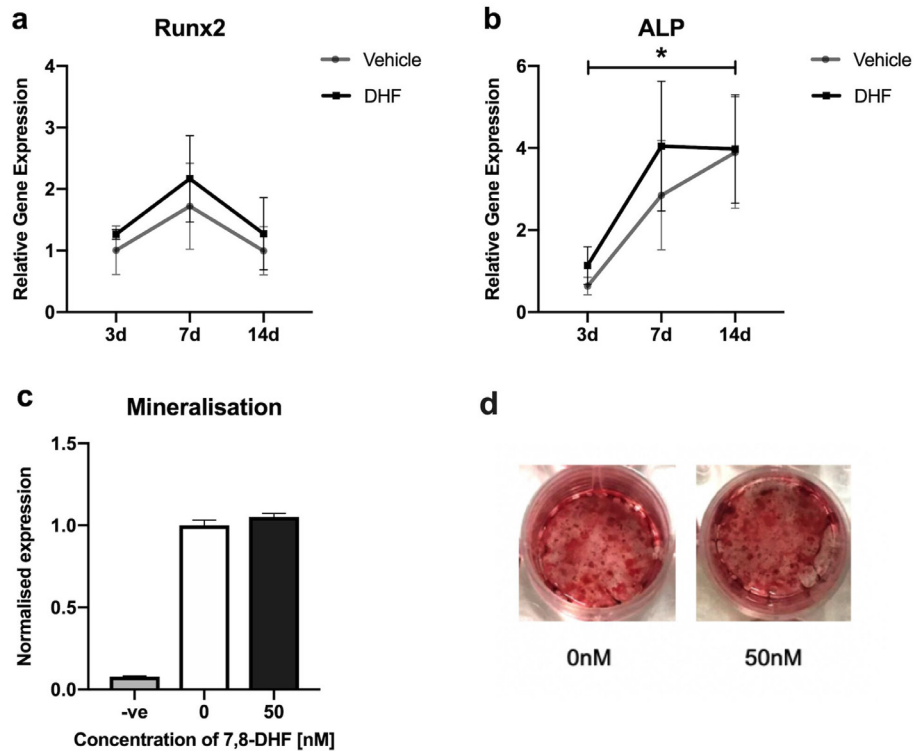
Figure 2. The effect of 7,8-DHF treatment in the osteoblastic mesenchymal cell line; Kusa4b10. There was no effect of time or 7,8-DHF on expression of Runx2 (a). For ALP expression (b), there was no effect of 7,8-DHF treatment; however, a main effect of time was found, with 14-day cells having greater ALP mRNA expression than 3-day cells (*p=0.041). Kusa4b10 cells formed mineral at 21 days of incubation; however, 7,8-DHF did not increase mineralization at any dose (c-d). Bars are mean ± SEM, n=6/group.

early osteoblasts[60], and alkaline phosphatase; a marker of mature osteoblasts[56].

Mineralization Analysis

For investigating the effects 7,8-DHF treatment has on osteoblastic cell mineralization, Kusa4b10 cells were cultured in osteoblastic differentiating medium treated with 0-, 10-, 50-, and 100nM of 7,8-DHF for 21 days (n=4/group). After 21 days, cells were stained with Alizarin red and inspected for mineralization nodules within the Kusa4b10 colonies. Kusa4b10 cells were washed three times in PBS, fixed in ice cold 70% ETOH for 30 min, and then stained with 0.5% Alizarin Red stain (pH 4.2) for 30 min. Cells were then washed five times in PBS and scanned images were taken. Mineralized areas were quantified using ImageJ software (National Institutes of Health, Bethesda, USA).

Statistical analysis

In vitro gene expression was analysed via two-way ANOVA, with Tukey's multiple comparisons conducted where appropriate. All other outcomes were analysed with Mann-Whitney U tests. Statistical analyses were performed using GraphPad Prism 8 software (GraphPad Software, Inc., USA), with significance defined as p<0.05.

Results

7,8-DHF reduces callus size

Representative µCT reconstruction of longitudinal mid-point hemi-calluses are shown in Figure 1a-b. Bony union was reached in all calluses by 28 days post-fracture in both the 7,8-DHF-treated and control groups. Analysis revealed the 7,8-DHF-treated group had a significant reduction in total tissue volume (Figure 1c; p=0.042), no change in fractional bone volume (Figure 1d; p=0.088), decreased mean polar moment of inertia (Figure 1e; p=0.004), and reduced mean cross-sectional area (Figure 1f; p=0.042) of callus compared to controls.

7,8-DHF reduces peak force to failure in fracture calluses

A three-point bending test was used to assess the biomechanical properties of 28-day tibial calluses. As seen in Table 2, calluses of mice treated with 7,8-DHF following fracture had a significantly decreased peak force to failure (p=0.011) compared to controls. Conversely, stiffness was increased in calluses of mice treated with 7,8-DHF when compared to vehicle-treated mice (p=0.012). There was no significant difference in cross-sectional area, bending stress, or Young's modulus between groups (Table 2).

Table 2. Mechanical properties of vehicle and 7,8-DHF-treated calluses at 28-day post-fracture.

Treatment	Peak force (N)	Stiffness (x 10^4 Nm^2)	CSA (x 10^{-6} m^2)	Bending stress (x 10^6 Nm^{-2})	YM (x 10^8 Nm^{-2})
Vehicle (n=12) Mean ± SEM	13.48 ± 0.84	9.38 ± 0.50	4.56 ± 0.30	3.84 ± 0.39	7.21 ± 1.18
7,8-DHF (n=9) Mean ± SEM	10.64 ± 0.51	13.01 ± 1.04	3.94 ± 0.29	3.75 ± 0.46	13.79 ± 2.96
p-value	* 0.011	*0.012	0.13	0.65	0.06

7,8-DHF, 7,8-dihydroxyflavone; CSA, cross-sectional area; YM, Young's modulus. Values are means ± SEM. *symbol indicates statistical significance (p<0.05) determined by a Mann-Whitney U tests.

7,8-DHF does not alter expression of osteoblastic markers in Kusa4b10 cells

Messenger RNA levels of osteoblastic markers Runx2 and alkaline phosphatase were quantified by RT-PCR in Kusa4b10 cells at 3-, 7-, and 14-days of differentiation. For Runx2 mRNA expression (Figure 2a), there was no main effect of treatment ($F_{(1,29)}$=0.613, p=0.440), no main effect of time ($F_{(2,29)}$=1.603, p=0.219), and no interaction of treatment and time ($F_{(1,29)}$=0.020, p=0.981). For ALP mRNA expression (Figure 2b), there was no main effect of treatment ($F_{(1,28)}$=0.371, p=0.547), a main effect of time ($F_{(2,28)}$=3.729, p=0.037), and no interaction of treatment and time ($F_{(1,28)}$=0.112, p=0.895). Post-hoc analysis revealed that ALP mRNA expression was increased in cells cultured for 14-days when compared cells cultured for 3-days (p=0.041).

7,8-DHF does not influence mineralization in Kusa4b10 cells

Mineralization nodules were detected at 21 days in Kusa4b10 cells at all concentrations (0, 10, 50, 100 nm) of 7,8-DHF treatment (Figures 2c-d). There were no apparent changes in the number of nodules or mineralization between the treatment groups or controls, and there was no mineralization evident in the negative control cultures of undifferentiated Kusa4b10s.

Discussion

Although BDNF and its TrkB receptors have been localized in healing fractures of mice, rats, and humans, the role of TrkB signalling in fracture healing is not well understood. Here it was hypothesised that TrkB agonism using the flavonoid, 7,8-DHF, would have positive effects on fracture healing, as measured by structural and biomechanical analysis. To the contrary, it was found that systemic administration of 5 mg/kg/day of 7,8-DHF for 14 days in mice with healing tibial fracture, resulted in mechanically weaker calluses with reduced bone and tissue volume. Furthermore, *in vitro* experiments revealed no effect of 7,8-DHF on osteoblastic differentiation and mineralization. Together, these data show that fracture healing was impaired by the 7,8-DHF treatment paradigm used in this study, and that TrkB activation may not directly increase osteoblastic bone formation.

µCT was used to investigate the influence of 7,8-DHF on the bone and callus content at 28 days post-fracture. Calluses of 7,8-DHF-treated animals were smaller than that of vehicle-treated animals, with reduced tissue volume and mean cross-sectional area. Additionally, µCT analyses revealed that 7,8-DHF treatment decreased the theoretical mean polar moment of inertia; a measurement of inherent rotational stiffness of bone[61] compared to controls. This finding was supported by three-point bending analysis, with peak-force to failure significantly reduced in the 7,8-DHF-treated mice compared to controls. Considered together, these findings indicate that 7,8-DHF negatively impacted healing of fractures, forming fractures that were both smaller in size and mechanically weaker.

Interestingly, the present findings are dissimilar to a study that investigated BDNF-functionalized cement treatment during femoral fracture healing in mice, which found BDNF treatment was beneficial to fracture healing[62]. Although *in vivo* bone formation was not directly assessed in the current study, that calluses were smaller and mechanically inferior likely indicates reduced callus bone formation in the 7,8-DHF-treated mice compared to controls[63]. One possible explanation for these contrasting findings may be due to differences in the biodistribution of the two treatments used in the studies, with 7,8-DHF previously shown to readily cross the blood brain barrier (BBB)[36,42-45], whereas exogenously applied BDNF is restricted to the peripheral circulation[64]. Previous experiments have shown peripheral BDNF has positive effects on bone[28,30,33], and central depletion of BDNF increases bone mineral density[65], highlighting the likely possibility BDNF has opposite, central and peripheral effects on bone, which are similar to those described for the hormone leptin[66,67].

Therefore, it is proposed in this study that 7,8-DHF's action on TrkB receptors occurred centrally in the brain and overrode possible positive peripheral effects on bone to negatively impact on fracture healing. A definitive study that investigated the selective deletion of BDNF in the brains of mice and its effect on bone phenotype[65], demonstrated in these centrally-deleted BDNF mice, there was an increase in femoral lengths, and an overall increase in bone mineral density (BMD) compared to wild type mice[65]. Therefore, suggested in the current experiments is the central activation

of TrkB receptors via 7,8-DHF, which in turn negatively impacted bone metabolism and resulted in smaller fracture calluses and weaker fracture sites.

Additionally, in the present study, an *in vitro* model, Kusa4b10, was used to determine the effects of 7,8-DHF on osteoblasts and bone mineralization. Kusa4b10 cells are a more osteogenic sub-clone of murine multipotential bone marrow stromal cell line, Kusa O[56]. Like Kusa O cells at day O, Kusa4b10 resemble an osteoprogenitor phenotype and by day 14 resemble a mature osteoblastic phenotype[56] and therefore are an ideal cell line to study regarding *in vitro* osteoblastic differentiation and mineralization. Our laboratory has previously localized TrkB receptors on parent line Kusa O, at day 14 of differentiation via Western blot (unpublished data). Likewise, TrkB receptors have also been localised in a murine osteoblastic precursor cells line, MC3T3-E1[34], which suggests a possible role for TrkB agonists on bone metabolism. This data is additionally supported *in vivo* rodent models and human fracture healing, which have localised TrkB receptors on chondrocytes and osteoblasts during bone growth and fracture healing[25,28]. In the current study, it was found that 3-, 7-, or 14-days of 7,8-DHF treatment to Kusa4b10 cells did not alter gene expression of Runx2 and ALP, which are two markers osteoblastic differentiation. The current findings are similar to a study that showed that BDNF administration did not alter ALP gene expression in MC3T3-E1 after 5 days of treatment[30]. However, in the same study, MC3TC-E1 had increased mineralization following BDNF treatment[30], whereas in the current study 7,8-DHF did not increase mineralization of Kusa4b10 cells at 21 days differentiation. Lack of difference in mineralization may be a result of the timepoint analysed. At 21 days, there was dense mineralization seen in controls and treated Kusa4b10, and had mineralization been analysed at an earlier timepoint, such as when the cells were just starting to form mineral there may have been a difference.

In summary, 5 mg/kg/day of 7,8-DHF treatment to mice with tibial fractures resulted in structurally smaller calluses and mechanically weaker fracture sites. It is proposed that 7,8-DHF acted centrally on TrkB receptors in the brain to negatively impact bone remodelling. The present findings suggest that BDNF has a role in bone remodelling, and we propose that there may be two opposing outcomes on bone remodelling depending if TrkB signalling pathways are activated in the central or peripheral nervous systems.

References

1. Nguyen ND, Ahlborg HG, Center JR, Eisman JA, Nguyen TV. Residual lifetime risk of fractures in women and men. J Bone Miner Res 2007;22(6):781-8.
2. Mills LA, Simpson AH. The relative incidence of fracture non-union in the Scottish population (5.17 million): a 5-year epidemiological study. BMJ Open 2013;3(2).
3. Zura R, Xiong Z, Einhorn T, Watson JT, Ostrum RF, Prayson MJ, et al. Epidemiology of Fracture Nonunion in 18 Human Bones. JAMA Surg 2016;151(11).
4. Einhorn TA, Gerstenfeld LC. Fracture healing: mechanisms and interventions. Nat Rev Rheumatol 2015;11(1):45-54.
5. Warden SJ, Bennell KL, McMeeken JM, Wark JD. Acceleration of fresh fracture repair using the sonic accelerated fracture healing system (SAFHS): a review. Calcif Tissue Int 2000;66(2):157-63.
6. Pounder NM, Harrison AJ. Low intensity pulsed ultrasound for fracture healing: a review of the clinical evidence and the associated biological mechanism of action. Ultrasonics 2008;48(4):330-8.
7. Leighton R, Watson JT, Giannoudis P, Papakostidis C, Harrison A, Steen RG. Healing of fracture nonunions treated with low-intensity pulsed ultrasound (LIPUS): A systematic review and meta-analysis. Injury 2017;48(7):1339-47.
8. Ghiasi MS, Chen J, Vaziri A, Rodriguez EK, Nazarian A. Bone fracture healing in mechanobiological modeling: A review of principles and methods. Bone Rep 2017;6:87-100.
9. Kermani P, Hempstead B. Brain-derived neurotrophic factor: a newly described mediator of angiogenesis. Trends Cardiovasc Med 2007;17(4):140-3.
10. Kermani P, Rafii D, Jin DK, Whitlock P, Schaffer W, Chiang A, et al. Neurotrophins promote revascularization by local recruitment of TrkB+ endothelial cells and systemic mobilization of hematopoietic progenitors. J Clin Invest 2005;115(3):653-63.
11. Raychaudhuri SK, Raychaudhuri SP, Weltman H, Farber EM. Effect of nerve growth factor on endothelial cell biology: proliferation and adherence molecule expression on human dermal microvascular endothelial cells. Arch Dermatol Res 2001;293(6):291-5.
12. Emanueli C, Salis MB, Pinna A, Graiani G, Manni L, Madeddu P. Nerve growth factor promotes angiogenesis and arteriogenesis in ischemic hindlimbs. Circulation 2002;106(17):2257-62.
13. Micera A, Lambiase A, Stampachiacchiere B, Bonini S, Levi-Schaffer F. Nerve growth factor and tissue repair remodeling: trkA(NGFR) and p75(NTR), two receptors one fate. Cytokine Growth Factor Rev 2007;18(3-4):245-56.
14. Werner S, Grose R. Regulation of wound healing by growth factors and cytokines. Physiol Rev 2003;83(3):835-70.
15. Scuri M, Samsell L, Piedimonte G. The role of neurotrophins in inflammation and allergy. Inflamm Allergy Drug Targets 2010;9(3):173-80.
16. Calabrese F, Rossetti AC, Racagni G, Gass P, Riva MA, Molteni R. Brain-derived neurotrophic factor: a bridge between inflammation and neuroplasticity. Front Cell Neurosci 2014;8:430.
17. Beamer B, Hettrich C, Lane J. Vascular endothelial growth factor: an essential component of angiogenesis and fracture healing. HSS J 2010;6(1):85-94.
18. Johnstone MR, Sun M, Taylor CJ, Brady RD, Grills BL, Church JE, et al. Gambogic amide, a selective TrkA agonist, does not improve outcomes from traumatic brain injury in mice. Brain Inj 2018;32(2):257-68.

19. Grills BL, Schuijers JA, Ward AR. Topical application of nerve growth factor improves fracture healing in rats. J Orthop Res 1997;15(2):235-42.

20. Wang L, Zhou S, Liu B, Lei D, Zhao Y, Lu C, et al. Locally applied nerve growth factor enhances bone consolidation in a rabbit model of mandibular distraction osteogenesis. J Orthop Res 2006;24(12):2238-45.

21. Huang EJ, Reichardt LF. Neurotrophins: roles in neuronal development and function. Annu Rev Neurosci 2001;24:677-736.

22. Reichardt LF. Neurotrophin-regulated signalling pathways. Philos Trans R Soc Lond B Biol Sci 2006;361(1473):1545-64.

23. Bothwell M. Functional interactions of neurotrophins and neurotrophin receptors. Annu Rev Neurosci 1995;18:223-53.

24. Barbacid M. The Trk family of neurotrophin receptors. J Neurobiol 1994;25(11):1386-403.

25. Kilian O, Hartmann S, Dongowski N, Karnati S, Baumgart-Vogt E, Hartel FV, et al. BDNF and its TrkB receptor in human fracture healing. Ann Anat 2014;196(5):286-95.

26. Ebadi M, Bashir RM, Heidrick ML, Hamada FM, Refaey HE, Hamed A, et al. Neurotrophins and their receptors in nerve injury and repair. Neurochem Int 1997;30(4-5):347-74.

27. Asaumi K, Nakanishi T, Asahara H, Inoue H, Takigawa M. Expression of neurotrophins and their receptors (TRK) during fracture healing. Bone 2000;26(6):625-33.

28. Yamashiro T, Fukunaga T, Yamashita K, Kobashi N, Takano-Yamamoto T. Gene and protein expression of brain-derived neurotrophic factor and TrkB in bone and cartilage. Bone 2001;28(4):404-9.

29. Aiga A, Asaumi K, Lee YJ, Kadota H, Mitani S, Ozaki T, et al. Expression of neurotrophins and their receptors tropomyosin-related kinases (Trk) under tension-stress during distraction osteogenesis. Acta Med Okayama 2006;60(5):267-77.

30. Ida-Yonemochi H, Yamada Y, Yoshikawa H, Seo K. Locally Produced BDNF Promotes Sclerotic Change in Alveolar Bone after Nerve Injury. PloS One 2017;12(1):e0169201.

31. Matsuda S, Fujita T, Kajiya M, Takeda K, Shiba H, Kawaguchi H, et al. Brain-derived neurotrophic factor induces migration of endothelial cells through a TrkB-ERK-integrin alphaVbeta3-FAK cascade. J Cell Physiol 2012;227(5):2123-9.

32. Lin CY, Hung SY, Chen HT, Tsou HK, Fong YC, Wang SW, et al. Brain-derived neurotrophic factor increases vascular endothelial growth factor expression and enhances angiogenesis in human chondrosarcoma cells. Biochem Pharmacol 2014;91(4):522-33.

33. Kajiya M, Shiba H, Fujita T, Ouhara K, Takeda K, Mizuno N, et al. Brain-derived neurotrophic factor stimulates bone/cementum-related protein gene expression in cementoblasts. J Biol Chem 2008;283(23):16259-67.

34. Nakanishi T, Takahashi K, Aoki C, Nishikawa K, Hattori T, Taniguchi S. Expression of nerve growth factor family neurotrophins in a mouse osteoblastic cell line. Biochem

35. Jang SW, Liu X, Yepes M, Shepherd KR, Miller GW, Liu Y, et al. A selective TrkB agonist with potent neurotrophic activities by 7,8-dihydroxyflavone. Proc Natl Acad Sci USA 2010;107(6):2687-92.

36. Agrawal R, Noble E, Tyagi E, Zhuang Y, Ying Z, Gomez-Pinilla F. Flavonoid derivative 7,8-DHF attenuates TBI pathology via TrkB activation. Biochim Biophys Acta 2015;1852(5):862-72.

37. Liu X, Chan CB, Jang SW, Pradoldej S, Huang J, He K, et al. A synthetic 7,8-dihydroxyflavone derivative promotes neurogenesis and exhibits potent antidepressant effect. J Med Chem 2010;53(23):8274-86.

38. Zhao S, Gao X, Dong W, Chen J. The Role of 7,8-Dihydroxyflavone in Preventing Dendrite Degeneration in Cortex After Moderate Traumatic Brain Injury. Mol Neurobiol 2016;53(3):1884-95.

39. Zhao S, Yu A, Wang X, Gao X, Chen J. Post-Injury Treatment of 7,8-Dihydroxyflavone Promotes Neurogenesis in the Hippocampus of the Adult Mouse. J Neurotrauma 2016;33(22):2055-64.

40. Gupta VK, You Y, Li JC, Klistorner A, Graham SL. Protective effects of 7,8-dihydroxyflavone on retinal ganglion and RGC-5 cells against excitotoxic and oxidative stress. J Mol Neurosci 2013;49(1):96-104.

41. Chen L, Gao X, Zhao S, Hu W, Chen J. The Small-Molecule TrkB Agonist 7, 8-Dihydroxyflavone Decreases Hippocampal Newborn Neuron Death After Traumatic Brain Injury. J Neuropathol Exp Neurol 2015;74(6):557-67.

42. Devi L, Ohno M. 7,8-dihydroxyflavone, a small-molecule TrkB agonist, reverses memory deficits and BACE1 elevation in a mouse model of Alzheimer's disease. Neuropsychopharmacology 2012;37(2):434-44.

43. Castello NA, Nguyen MH, Tran JD, Cheng D, Green KN, LaFerla FM. 7,8-Dihydroxyflavone, a small molecule TrkB agonist, improves spatial memory and increases thin spine density in a mouse model of Alzheimer disease-like neuronal loss. PloS One 2014;9(3).

44. Zeng Y, Liu Y, Wu M, Liu J, Hu Q. Activation of TrkB by 7,8-dihydroxyflavone prevents fear memory defects and facilitates amygdalar synaptic plasticity in aging. J Alzheimers Dis 2012;31(4):765-78.

45. Andero R, Daviu N, Escorihuela RM, Nadal R, Armario A. 7,8-dihydroxyflavone, a TrkB receptor agonist, blocks long-term spatial memory impairment caused by immobilization stress in rats. Hippocampus 2012;22(3):399-408.

46. Scheller KJ, Williams SJ, Lawrence AJ, Djouma E. The galanin-3 receptor antagonist, SNAP 37889, suppresses alcohol drinking and morphine self-administration in mice. Neuropharmacology 2017;118:1-12.

47. Scheller KJ, Williams SJ, Lawrence AJ, Jarrott B, Djouma E. An improved method to prepare an injectable microemulsion of the galanin-receptor 3 selective antagonist, SNAP 37889, using Kolliphor((R)) HS 15. MethodsX 2014;1:212-6.

48. Johnstone MR, Brady RD, Schuijers JA, Church JE,

Biophys Res Commun 1994;198(3):891-7.

Orr D, Quinn JMW, et al. The selective TrkA agonist, gambogic amide, promotes osteoblastic differentiation and improves fracture healing in mice. J Musculoskelet Neuronal Interact 2019;19(1):94-103.

49. Yang Y, Salayandia VM, Thompson JF, Yang LY, Estrada EY, Yang Y. Attenuation of acute stroke injury in rat brain by minocycline promotes blood-brain barrier remodeling and alternative microglia/macrophage activation during recovery. J. Neuroinflammation 2015;12:26.

50. Singleton RH, Yan HQ, Fellows-Mayle W, Dixon CE. Resveratrol attenuates behavioral impairments and reduces cortical and hippocampal loss in a rat controlled cortical impact model of traumatic brain injury. J Neurotrauma 2010;27(6):1091-9.

51. Brady RD, Grills BL, Church JE, Walsh NC, McDonald AC, Agoston DV, et al. Closed head experimental traumatic brain injury increases size and bone volume of callus in mice with concomitant tibial fracture. Sci Rep 2016;6:34491.

52. Shultz SR, Sun M, Wright DK, Brady RD, Liu S, Beynon S, et al. Tibial fracture exacerbates traumatic brain injury outcomes and neuroinflammation in a novel mouse model of multitrauma. J Cereb Blood Flow Metab 2015;35(8):1339-47.

53. Brady RD, Grills BL, Romano T, Wark JD, O'Brien TJ, Shultz SR, et al. Sodium selenate treatment mitigates reduction of bone volume following traumatic brain injury in rats. J Musculoskelet Neuronal Interact 2016;16(4):369-76.

54. Brady RD, Shultz SR, Sun M, Romano T, van der Poel C, Wright DK, et al. Experimental Traumatic Brain Injury Induces Bone Loss in Rats. J Neurotrauma 2016;33(23):2154-60.

55. Sun M, Brady RD, Wright DK, Kim HA, Zhang SR, Sobey CG, et al. Treatment with an interleukin-1 receptor antagonist mitigates neuroinflammation and brain damage after polytrauma. Brain Behav Immun 2017;66:359-71.

56. Allan EH, Ho PW, Umezawa A, Hata J, Makishima F, Gillespie MT, et al. Differentiation potential of a mouse bone marrow stromal cell line. J Cell Biochem 2003;90(1):158-69.

57. Allan EH, Hausler KD, Wei T, Gooi JH, Quinn JM, Crimeen-Irwin B, et al. EphrinB2 regulation by PTH and PTHrP revealed by molecular profiling in differentiating osteoblasts. J Bone Miner Res 2008;23(8):1170-81.

58. Onan D, Allan EH, Quinn JM, Gooi JH, Pompolo S, Sims NA, et al. The chemokine Cxcl1 is a novel target gene of parathyroid hormone (PTH)/PTH-related protein in committed osteoblasts. Endocrinology 2009;150(5):2244-53.

59. Quach JM, Walker EC, Allan E, Solano M, Yokoyama A, Kato S, et al. Zinc finger protein 467 is a novel regulator of osteoblast and adipocyte commitment. J Biol Chem 2011;286(6):4186-98.

60. Nakashima K, Zhou X, Kunkel G, Zhang Z, Deng JM, Behringer RR, et al. The novel zinc finger-containing transcription factor osterix is required for osteoblast differentiation and bone formation. Cell 2002;108(1):17-29.

61. Turner CH, Burr DB. Basic biomechanical measurements of bone: a tutorial. Bone 1993;14(4):595-608.

62. Kauschke V, Schneider M, Jauch A, Schumacher M, Kampschulte M, Rohnke M, et al. Effects of a Pasty Bone Cement Containing Brain-Derived Neurotrophic Factor-Functionalized Mesoporous Bioactive Glass Particles on Metaphyseal Healing in a New Murine Osteoporotic Fracture Model. Int J Mol Sci 2018;19(11).

63. Doblare M, Garcia JM. On the modelling bone tissue fracture and healing of the bone tissue. Acta Cient Venez 2003;54(1):58-75.

64. Pilakka-Kanthikeel S, Atluri VS, Sagar V, Saxena SK, Nair M. Targeted brain derived neurotropic factors (BDNF) delivery across the blood-brain barrier for neuro-protection using magnetic nano carriers: an in-vitro study. PloS One 2013;8(4).

65. Camerino C, Zayzafoon M, Rymaszewski M, Heiny J, Rios M, Hauschka PV. Central depletion of brain-derived neurotrophic factor in mice results in high bone mass and metabolic phenotype. Endocrinology 2012;153(11):5394-405.

66. Khosla S. Leptin-central or peripheral to the regulation of bone metabolism? Endocrinology 2002; 143(11):4161-4.

67. Upadhyay J, Farr OM, Mantzoros CS. The role of leptin in regulating bone metabolism. Metabolism 2015;64(1):105-13.